JOURNAL OF GEOPHYSICAL RESEARCH, VOL. 103, NO. A9, PAGES 20,459-20,468, SEPTEMBER 1, 1998

Low-frequency impulsive auroral hiss observations at high geomagnetic latitudes

J. LaBelle, [1] A. T. Weatherwax, [2] J. Perring, [1] E. Walsh, [1] M. L. Trimpi, [1] and U.S. Inan [3]

Abstract.
Wave receivers in Antarctic Automatic Geophysical Observatories (AGOs) measure spectral features of low-frequency impulsive auroral hiss emissions which cannot be observed at northern hemisphere sites or near manned Antarctic stations due to man-made interference. From observations at AGO-P1 ($\sim$ 80° invariant latitude) we distinguish two spectral types of LF impulsive auroral hiss: normal events, in which the power spectral density is a decreasing function of frequency throughout the LF band, presumably peaking in the VLF band below the frequency range of the LF/MF/HF receiver; and LF cutoff events, for which the power spectral density peaks in the LF band with little or no power at VLF. Out of a large sample of impulsive auroral hiss events observed at AGO-P1, 64% are the normal type, 14% are the LF-cutoff type, and 22% are a mixture of both. A hiss propagation model similar to that of *Makita* [1979] was used to evaluate approximately whether the observed occurrence statistics of LF cutoff auroral hiss are consistent with previous models of auroral hiss generation and propagation. The results indicate that LF cutoff auroral hiss can be explained by propagation effects and suggest that the observed LF cutoff occurrence statistics are consistent with LF impulsive auroral hiss originating at or ducted to altitudes of 2000-5000 km.

1. Introduction

Despite its extensive application for communications, the LF/MF/HF band (30 kHz to 30 MHz) remains relatively little studied for sources of natural radio emissions detectable at ground level. Auroral radio emissions in this band include continuous and impulsive auroral hiss (reviews by *Helliwell* [1965]; *Makita* [1979], and *Sazhin et al.* [1993]), $2f_{ce}$- and $3f_{ce}$-auroral roar [*Kellogg and Monson*, 1979; *Weatherwax et al.*, 1993], and auroral MF burst [*Weatherwax et al.*, 1994a; *LaBelle et al.*, 1997]. Auroral hiss has been known longest and is the best understood of these phenomena. The continuous type usually lasts the order of an hour or more and is restricted to VLF. The impulsive type occurs during substorm onsets, consists of bursts of impulsive emissions lasting from a few seconds to tens of minutes, and often extends into the LF range [e.g., *Dowden*, 1959; *Morgan*, 1977a]; for example, *Jorgensen* [1968] reports observations of impulsive LF hiss exceeding 500 kHz at Byrd Station, Antarctica (-71° invariant). Modern wave receivers in Antarctica and elsewhere detect auroral hiss at frequencies exceeding 1 MHz. While much auroral hiss may be explained as coherent amplification by auroral electrons of whistler mode waves propagating at low phase velocities on the part of the whistler dispersion surface called the resonance cone [*Maggs*, 1976], there exist observations in space which cannot be completely explained by this model [e.g., *Morioka and Oya*, 1985; *Ergun et al.*, 1991].

The propagation characteristics of VLF and LF waves in the ionosphere significantly affect ground-based observations of auroral hiss. In particular, the wave vectors of the whistler mode auroral hiss in the ionosphere must be close to vertical in order to couple to the free-space mode in the underlying atmosphere. This requirement suggests that the hiss originates at altitudes where its frequency is close to the local electron gyrofrequency or plasma frequency, because in that frequency range the whistler mode waves on the resonance cone have wave vectors nearly parallel to the magnetic field and hence nearly vertical in the auroral ionosphere [e.g., *Maggs*, 1976]. The source altitudes of LF auroral hiss would therefore range from 1000 km (f_{pe} or $f_{ce} \approx$ 1 MHz) to 10000 km (f_{pe} or $f_{ce} \approx$ 30 kHz). On the basis of extensive observations of auroral hiss at Syowa Station, Antarctica (-70.4° invariant), *Makita*

[1]Department of Physics and Astronomy, Dartmouth College, Hanover, New Hampshire.
[2]Institute for Physical Science and Technology, University of Maryland, College Park, Maryland.
[3]Department of Electrical Engineering, Stanford University, Stanford, California.

Paper number 98JA01562.
0148-0227/98/98JA-01562$09.00

[1979] suggests that VLF continuous auroral hiss is generated at very high altitudes and ducted down to altitudes of a few thousand kilometers by magnetospheric denisty irregularities, while LF impulsive auroral hiss is generated at lower altitudes but may also be ducted along density irregularities or horizontal density gradients to lower altitudes before propagating nonducted to the ground. However, the source altitudes of the types of auroral hiss observed on the ground have not been established with certainty, and the conditions for which the auroral hiss reaches the ground have not been studied in detail, particularly at LF. Despite decades of study, these and other outstanding questions persist regarding the sources and propagation of auroral hiss observed at ground-level.

LF auroral hiss observations in Antarctica are of particular interest, because only in the remote Antarctic can ground-based instruments detect natural LF signals without significant interference from LF and AM broadcast signals, which dominate northern hemisphere observations. Dartmouth College operates LF/MF/HF receivers at South Pole Station and at several Automatic Geophysical Observatories in Antarctica. This paper explores whether measurements at these observatories can be used to test existing models of auroral hiss propagation.

2. Data Presentation

Dartmouth College has developed an LF/MF/HF receiver for the United States Antarctic Program Automatic Geophysical Observatories [*Rosenberg and Doolittle*, 1994]. The sensor is a magnetic loop placed 500 feet from the observatories. The receiver, which meets severe environmental, power, and data storage specifications, samples 100 frequencies between 30 kHz and 5 MHz each 10 s. The frequencies are not sampled monotonically in frequency but are interleaved so that broadband spectral features are measured with an effective 2.5 s time resolution. The receiver dynamic range is 70 dB. The smallest observable signal is approximately 5–10 nT/$\sqrt{\text{Hz}}$, but locally generated interference lines at discrete frequencies sometimes exceed that level by 20–40 dB. However, the overall level of man-made noise at the Antarctic AGO sites is significantly less than at northern hemisphere sites or at the manned Antarctic Stations [*Weatherwax et al.*, 1994b]. This reduction in background noise is particularly significant for the LF and MF bands (30–3000 kHz), large parts of which are unobservable in the Northern hemisphere due to AM and LF broadcast bands.

The LF/MF/HF receiver was installed in January, 1994, in AGO-P1 (83.86° S, 129.61° W geographic; 80.14° invariant), and continuous data are available from this station for the interval January 1994–March 1995. Supporting data are available from other AGO instruments including a VLF receiver which measured frequencies below 40 kHz, a vector flux-gate magnetometer, a search coil magnetometer sensitive to ULF waves, an imaging riometer, and an optical all-sky imager.

Figure 1 shows an example of an LF impulsive auroral hiss event recorded during 2235–2340 UT (1850–1955 MLT) on May 11, 1994, in the dusk to premidnight magnetic local time sector. Also shown is a voltage level proportional to the amplitude of 2–4 kHz EM waves measured with the VLF receiver, the H component of the geomagnetic field measured with the flux-gate magnetometer, and the corresponding geomagnetic fluctuations measured with the search coil magnetometer. The onset of micropulsations and a bay in the H component indicate a substorm onset at 2320 UT. The 2–4 kHz record shows signs of enhanced VLF waves during the entire interval, especially after 2245 UT. In contrast, the LF/MF/HF receiver detects significant LF hiss up to 500 kHz only during a five-minute interval (2320–2325 UT), except for possible brief occurrences near 2308 and 2318 UT which extend only up to about 200 kHz. In addition, the LF receiver detects auroral MF burst on 1500–2500 kHz starting at 2320 UT. We identify the LF signal below 500 kHz as impulsive auroral hiss based on its bursty nature, its association with substorm onset, and its association with MF burst and VLF waves. It is not unusual to detect auroral hiss at VLF over a much greater time interval than at LF; the power spectral density of auroral hiss usually peaks in the VLF range and decreases with increasing frequency above a few kilohertz, so it can easily exceed the VLF instrument threshold but lie below the threshold of the LF/MF/HF receiver.

Figure 2 shows bursts of VLF and LF impulsive auroral hiss observed at AGO-P1 during 0000–0600 UT (2015–0215 MLT) on May 30, 1994, corresponding to the nightside/midnight magnetic local time sector. The top panel shows a spectrogram of received LF signals, the middle panel shows the a voltage proportional to the amplitude of 30–40 kHz EM waves measured with the VLF receiver, and the bottom panel shows one component of the ULF geomagnetic fluctuations measured with the search coil magnetometer. Impulsive auroral hiss is observed at VLF or LF starting at 0045–0100 UT and 0505–0515 UT, and the search coil detects geomagnetic activity at these same times. The LF/MF/HF receiver detects auroral roar emissions at 2.8 MHz during and slightly preceding another interval of geomagnetic activity near 0245–0345 UT.

The impulsive auroral hiss events in Figure 2 illustrate two spectral types. The event at 0045-0200 is primarily of the "normal" type, in which the peak intensity is at VLF frequencies, below the range of the LF/MF/HF receiver. During 0045–0105 and 0145–0200 UT, the hiss occurs only in the VLF record; between 0105 and 0145 UT, both LF and VLF impulsive emissions are detected. For a short time around 0120–0125 UT, the second spectral type occurs, called "LF cutoff," in which the dominant waves are at frequencies above 100 kHz, and VLF waves are weak or absent. The 0510 UT impulsive auroral hiss event consists mostly of the LF cutoff type, with the most intense emissions at 200–250 kHz, except for one spike in the middle of the event which is registered by the 30–40 kHz VLF sig-

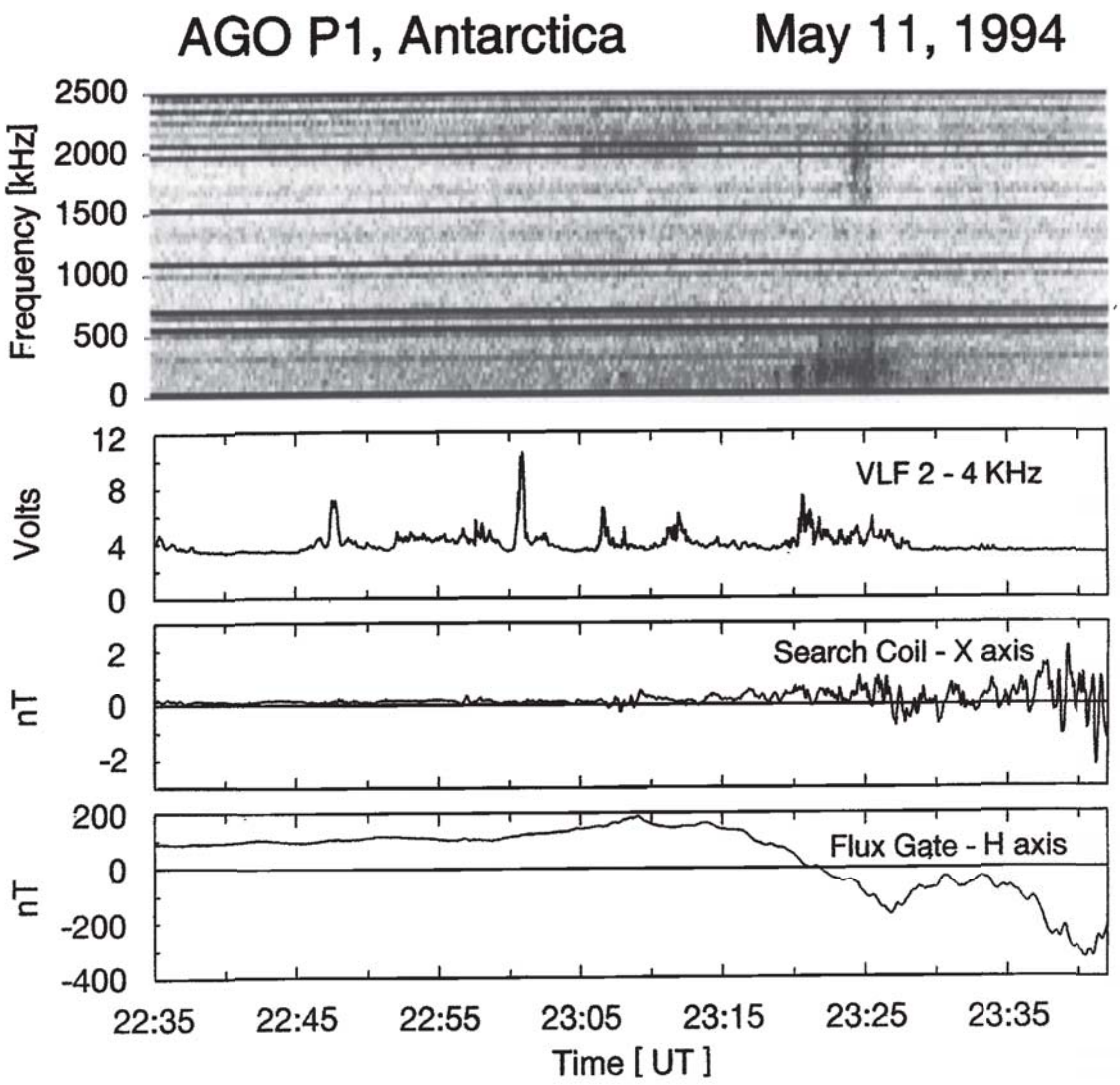

Figure 1. Spectrogram of 0–2.5 MHz radio waves recorded at AGO-P1 during 2235–2340 UT (1850–1955 MLT) on May 11, 1994. Auroral hiss and MF burst occur during the interval 2320–2327 UT. Also shown are the integrated power at 2–4 kHz measured with the VLF receiver, the H component of the geomagnetic field measured with the fluxgate magnetometer, and the corresponding geomagnetic fluctuations measured with the search coil magnetometer. For the VLF data, full scale (12 Volts) corresponds to 37 μV/m.

nal. Although both events in Figure 2 represent a mix of spectral types, the early 0100–0130 event consists primarily of the normal spectral type, while the later 0510 event consists primarily of the LF cutoff type. The LF/MF/HF receiver data provide a particularly effective means of detecting LF cutoff auroral hiss, but the phenomenon has been reported previously: for example, *Morgan* [1977*b*] reports that in many impulsive auroral hiss events detected at Frobisher Bay ($\sim 75°$ magnetic latitude), the low-frequency cutoff is too high to be observed on audio frequency records.

Figure 3 provides more examples of these two spectral types of impulsive auroral hiss, recorded during 1600–2400 UT (1215–2015 MLT) on January 2, 1995, in the noon to dusk magnetic local time sector. Several impulsive auroral hiss events appear in the 30–1200 kHz LF spectrogram (top panel) and 30–40 kHz wave amplitude (second panel). Impulsive auroral hiss emissions at 1640 and 1950–2000 UT are LF cutoff types, while hiss emissions during 2135–2235 UT are the normal type, and those during 1650–1720 UT are mixed. The bottom three panels present an expanded view of 1630–1740 UT. The most intense impulsive hiss emissions at 1659, 1703, and 1705 UT are the normal type. The 2–3 min modulation in the intensity of the impulsive auroral hiss may be related to simultaneous fluctuations in the geomagnetic field shown in the bottom panel.

From inspection of daily survey plots of AGO-P1 LF/MF/HF data between January 1994 and March 1995, supplemented with specially produced plots of expanded resolution when needed, we generated a database of 181 impulsive LF impulsive auroral hiss events

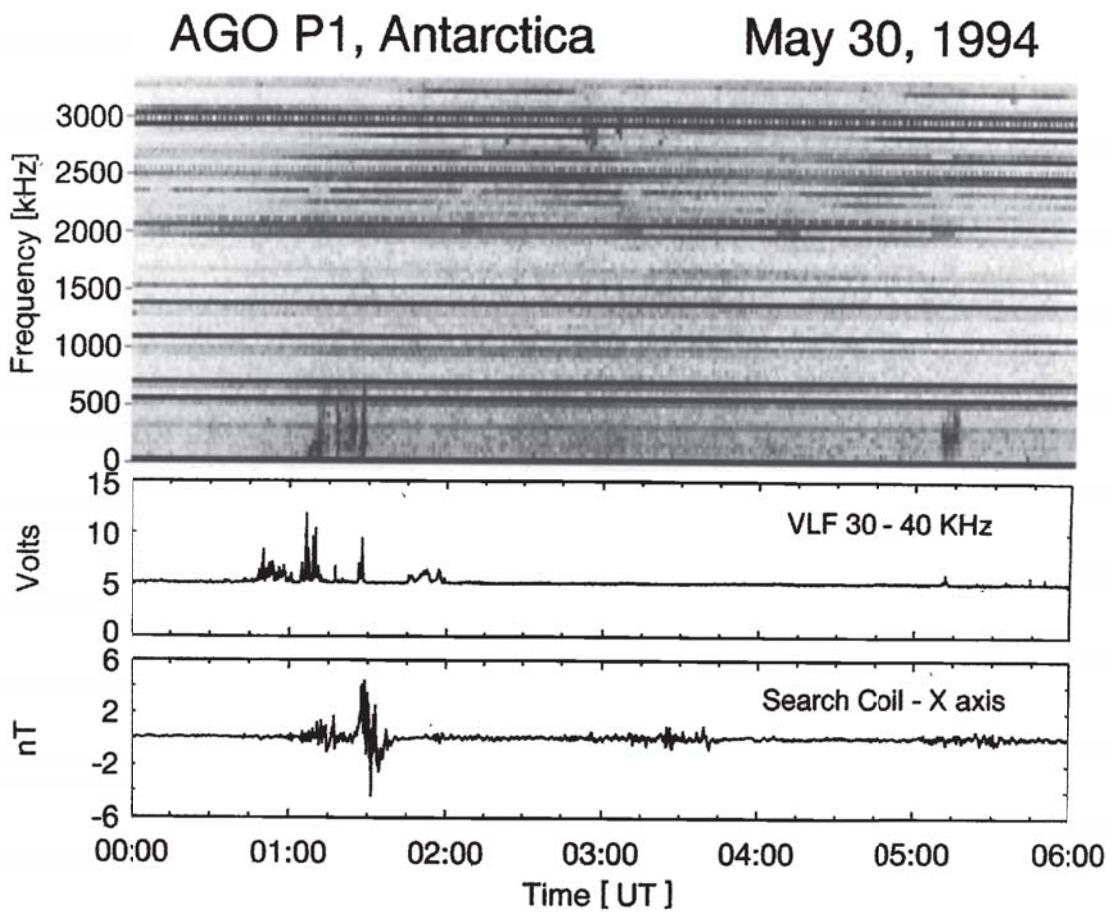

Figure 2. LF auroral hiss observed simultaneously at AGO-P1 with the Dartmouth LF/MF/HF receiver (top panel) and the Stanford VLF receiver (second panel) during 0000-0600 UT (2015–0215 MLT) on May 30, 1994. For the VLF data, full scale (15 Volts) corresponds to 54 μV/m. The search coil (bottom panel) records fluctuations in the geomagnetic field during the times when impulsive auroral hiss is observed. The LF/MF/HF receiver also detects auroral roar emissions at 2.8 MHz during 0245–0345 UT.

exceeding 30 nV/m$\sqrt{\text{Hz}}$ (intense events) and 423 events in the range 10–30 nV/m$\sqrt{\text{Hz}}$ (medium events). A far greater number of weak events (< 10 nV/m$\sqrt{\text{Hz}}$) occur, not included in the data base. Bursts of impulsive auroral hiss had to occur ten minutes apart in order to count as separate events. While identifying LF hiss events, a parallel data base was accumulated containing all time intervals when LF auroral hiss exceeding 10 nV/m$\sqrt{\text{Hz}}$ was not observable, due to various effects such as broadcast band interference, snow-static, or lack of data. The hours when auroral hiss was not observable were used to normalize the occurrence statistics of the impulsive auroral hiss, which we present in units of hiss events per hour of valid data.

Figure 4a shows the diurnal variation of the occurrence rate, based on the 604 events in our database. Error bars indicate the 1σ uncertainty level calculated based on statistical considerations. The occurrence rate of LF impulsive auroral hiss peaks in the pre-midnight hours (magnetic local time), consistent with previous observations of LF hiss [*Morgan*, 1977a, Figure 3] and VLF hiss [e.g., *Jorgensen*, 1966; *Makita*, 1979]. Figure 4b shows the seasonal variation of the occurrence rate. The peak in austral winter (June/July) is consistent with previous observations, but the weak secondary peak in the occurrence rate in January 1994 during the conjugate hemisphere winter was not observed by *Makita* [1979] at VLF frequencies at Syowa Station [*Makita*, 1979, Figure 12b]. This secondary peak does not recur in the 1994–1995 austral summer, however. (As the error bars indicate, the weak peak in occurrence rate during December 1994 is not significant in relation to that recorded in January 1994.) Such a conjugate winter peak in the occurrence rate would be surprising since previous observations at auroral latitudes in Antarctica and Iceland indicate that VLF auroral hiss occurs rarely and weakly at ground level in the conjugate hemisphere during the solstice periods, presumably because of absorption in the daylit ionosphere [*Sato et al.*, 1987]. Future AGO data will show whether a secondary peak in the impulsive auroral hiss occurrence rate observed at high latitude is a persistent or occa-

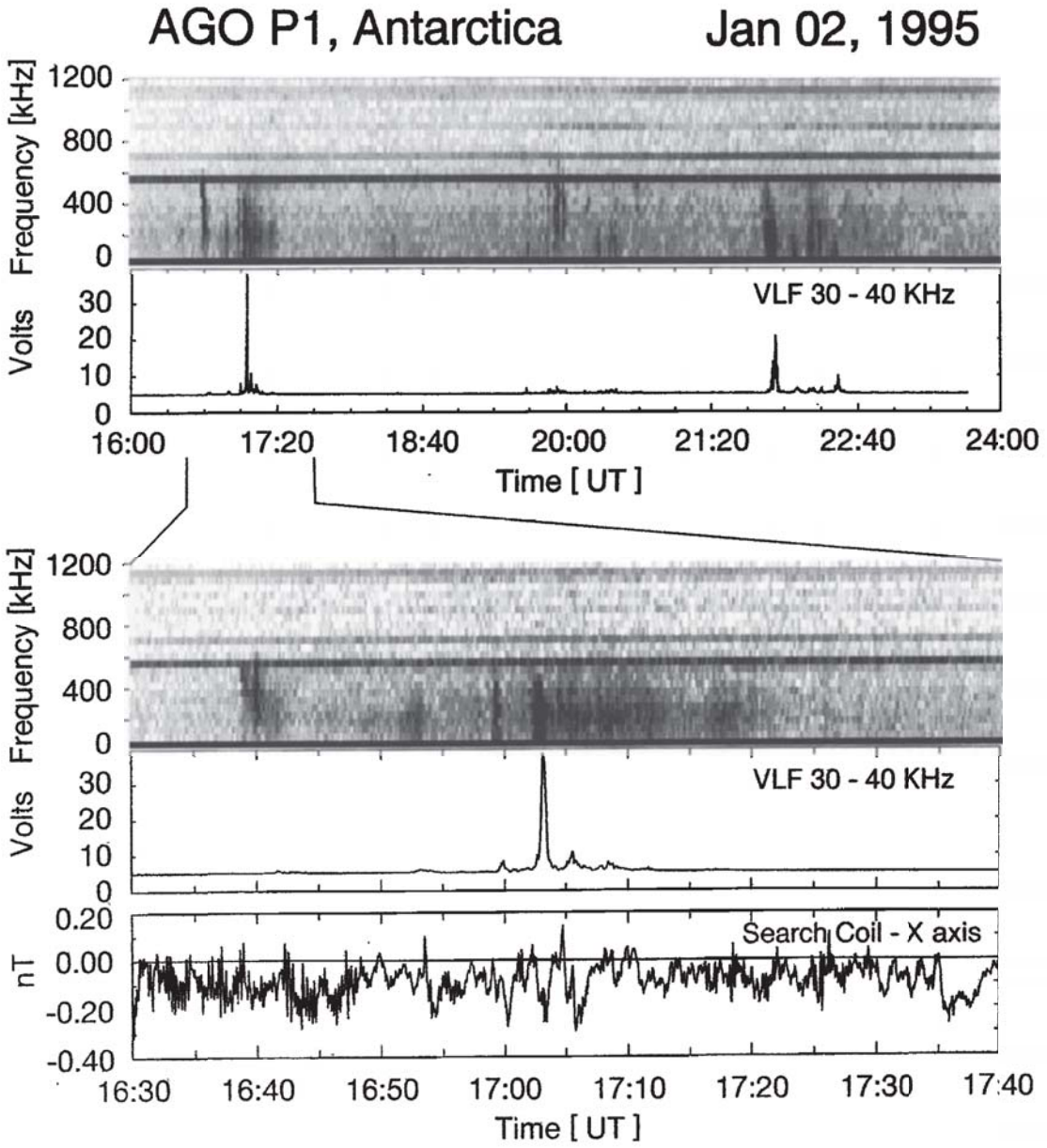

Figure 3. Auroral hiss recorded at AGO-P1 during 1600–2400 UT (1215–2015 MLT) on January 2, 1995. Several impulsive auroral hiss events appear in the 30–1200 kHz LF spectrogram (top panel) and VLF wave power integrated over 30-40 kHz (second panel). Those at 1640 and 1950–2000 UT are LF cutoff types, while those at 2135–2235 UT are the normal type, and those at 1650–1720 UT are mixed. The bottom three panels present an expanded view of the 1630–1740 UT interval, including the search coil x component which measured fluctuations in the geomagnetic field at the time of the most intense auroral hiss emissions. For the VLF data, full scale (40 Volts) corresponds to 144 μV/m.

sional feature and will allow a better assessment of its statistical significance.

From the database of LF impulsive auroral hiss events detected at AGO-P1 in 1994–1995, 261 randomly selected events were inspected in detail and identified as normal, LF cutoff or mixed spectral types. Of these 261 events, 168 (64%) are the normal type, 36 (14%) are the LF cutoff type, and 57 (22%) are a mixture of both types. These statistics show that at AGO-P1, approximately one third of the sampled LF hiss events are entirely or partly the LF cutoff type. Of course, if VLF hiss events were included in the sample, the proportion of LF cutoff events would be lower, because the sample would be considerably enlarged by events which are observable at VLF but not at LF.

Figure 5a shows an individual spectrum of LF cutoff auroral hiss recorded at 0515 UT on May 30, 1994, corresponding to the second impulsive auroral hiss event

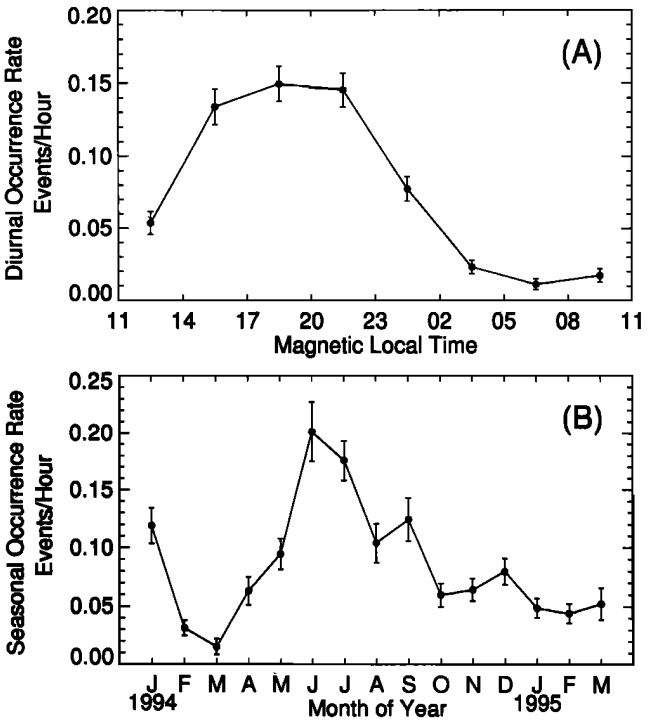

Figure 4. Diurnal and Seasonal occurrence rates of LF auroral hiss emissions recorded at AGO-P1 between January 1994 and March 1995. Error bars indicate the 1σ uncertainty levels inferred from statistical considerations. The occurrence rate peaks in the premidnight evening hours and during the austral winter. A weak secondary peak in the occurrence rate during January 1994 did not repeat in 1995.

shown in Figure 2. In this example, the spectrum peaks near 150 kHz, and the power spectral density at 50 kHz is lower by a factor of $\approx$ 16. Such spectral measurements provide an estimate of the lower cutoff frequency of LF cutoff auroral hiss, with two limitations: first, the resolution of the receiver is 10 kHz, so the identification of the cutoff is no better than that; second, the lowest frequency detected by the receiver is 30 kHz, so it is only possible to identify LF cutoff events with cutoff frequencies exceeding 40–50 kHz. Figure 5b shows the distribution of cutoff frequencies determined from measuring 45 randomly selected LF cutoff or mixed auroral hiss events. In this analysis the cutoff is defined as the half-power point below the peak in the spectrum. The measured cutoffs range from 50 kHz, the instrumental lower bound, to 330 kHz. The number of examples is largest for the lowest frequency bin and drops off steeply with increasing frequency. Since auroral hiss observed at ground level exhibits a low-frequency cutoff, usually at VLF, we interpret the distribution in Figure 5 as the tail of a more comprehensive distribution of cutoffs which peaks at VLF below the range of the LF/MF/HF receiver. The peak power spectral density of LF cutoff events occurs at a few hundred kHz, similar to auroral kilometric radiation (AKR). However, satellite observations made at great distances from the Earth show that the lower cutoff of AKR is more commonly at 100 kHz or more, and AKR events which cutoff at lower frequencies are rarer the lower the cutoff frequency. This trend is opposite to that shown in Figure 5 for LF cutoff auroral hiss. On the other hand, it is well-known that auroral hiss observed at ground level exhibits a low-frequency cutoff, with VLF hiss being more commonly observed than LF hiss, which agrees with the trend shown in Figure 5. Therefore Figure 5 strongly suggests that LF cutoff events are associated with auroral hiss rather than AKR, as would also be concluded from the case studies presented in Figures 1–3.

3. Modeling LF Cutoff Auroral Hiss

Maggs [1976] worked out the details of a theory in which auroral hiss is generated by convective amplification of whistler mode waves in an auroral electron beam. The whistler mode waves must have low phase velocities in order to interact with the beam, which re-

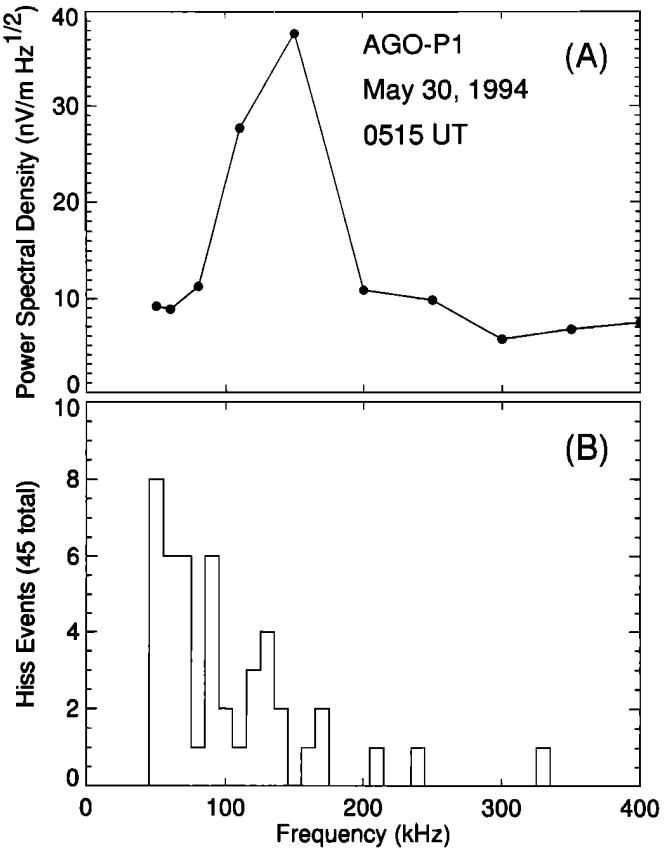

Figure 5. (a) An example spectrum of LF cutoff impulsive auroral hiss recorded at 0515 UT on May 30, 1994, corresponding to the second impulsive auroral hiss event shown in Figure 2. (b) The distribution of cutoff frequencies determined from 45 randomly selected LF cutoff type auroral hiss events. The measured cutoffs range from 50 kHz, the instrumental lower bound, to 330 kHz. The number of examples peaks in the lowest-frequency bin and drops off steeply with increasing frequency.

quires them to propagate on the resonance cone portion of the whistler dispersion surface. In this regime, higher whistler mode frequencies have more oblique group velocities and more parallel phase velocities than lower frequencies, which results in a saucer-shaped emission observed by satellites flying over or under a discrete source, whose altitude can be inferred from features of the saucer [e.g., *Mosier and Gurnett*, 1969]. *Yamamoto* [1979] extends this model by looking at the dependence of auroral hiss intensity on altitude and on the electron beam energy; he suggests that continuous hiss may result from low beam energies, in which case the waves are generated at high altitudes and at VLF, while impulsive hiss is generated over a wider range of altitudes when the electron beam has greater energy. Though this mechanism may provide a satisfactory explanation for the generation of auroral hiss, the source altitude of auroral hiss observed on the ground remains not well established because propagation effects and the condition for the waves to couple into the atmosphere play significant roles in determining whether auroral hiss from a particular source can be detected on the ground. Previous comparisons between ground-based and in situ measurements of auroral hiss have not provided sufficient cases to answer this question.

Because auroral hiss wave vectors in the ionosphere must be close to vertical in order for the waves to couple into the atmosphere, hiss observed at ground level may originate at altitudes where its frequency is close to the local electron gyrofrequency or plasma frequency, because in this frequency range the resonant whistler mode waves have wave vectors nearly parallel to the magnetic field and hence nearly vertical in the auroral ionosphere. The source altitudes of LF impulsive auroral hiss would therefore range from 1000 km (f_{pe} or $f_{ce} \approx 1$ MHz) to 10,000 km (f_{pe} or $f_{ce} \approx 30$ kHz). *Makita* [1979] suggests an altitude range of 5000–30000 km for 2–100 kHz impulsive auroral hiss. *Makita*'s [1979] ground-based observations suggest that VLF continuous auroral hiss is generated at very high altitudes and ducted to a few thousand kilometers altitude by density irregularities; this model explains how the waves get from a distant source to the ground with arrival bearings confined to field lines near the optical aurora, and it is supported by direction finding measurements of VLF auroral hiss at Syowa Station (69.03° S, 39.60° W, 70.4° invariant) which show that the auroral hiss emerges from a region several hundred kilometers equatorward of the optical auroral forms [*Makita*, 1979]. LF impulsive auroral hiss is generated at lower altitudes but may also be ducted along density irregularities or horizontal density gradients to lower altitudes before propagating nonducted to the ground.

To determine whether the statistics of LF cutoff auroral hiss measured at AGO-P1 are consistent with this scenario, we explore a quantitative physical model for the propagation of the auroral hiss from source to ground developed by *Makita* [1979]. A similar model has been applied to low-latitude hiss by *Singh and Singh* [1978, and references therein]. The model starts by launching whistler mode waves at a height h, which may be taken either as the source height of the auroral hiss or as duct-exit altitude, where hiss propagating downward in a field-aligned duct from a higher-altitude source becomes nonducted. For this rough preliminary calculation, we assume that the 40–80 kHz components of the hiss originate or become nonducted at approximately the same altitude.

After the auroral hiss is generated or emerges from the duct, we follow its propagation down to 200 km altitude using a magnetospheric ray-tracing code developed at Stanford [*Burtis*, 1974; *Inan and Bell*, 1977] based on pioneering early work by *Kimura* [1966] and others. Several parameters in the code allow the user to set the electron density at the F peak and a polynomial dependence for the decrease in electron density with altitude above the F peak. For all runs shown below, the density at the F peak was set to 5×10^4 cm^{-3} (plasma frequency of 2 MHz). The code assumes a dipole magnetic field. Waves are launched at prescribed wave normal angles at the source height h described above. The ray-tracing step size is a variable parameter but is set to be small enough that smaller step sizes do not significantly affect the result. The output is a sequence of rays at all altitudes down to 200 km, including in particular the angles that each ray makes with the vertical at the 200 km end point of the ray trace.

For the final step, the ionosphere-atmosphere interface is modeled as a plane boundary, with the index of refraction equal to unity in the atmosphere and given by the whistler mode value in the ionosphere:

$$n^2 = \frac{f_{pe}^2}{(f f_{ce} \cos\theta - f^2)} \tag{1}$$

where f is the frequency of the whistler mode wave; f_{pe} is the plasma frequency, taken to be 2 MHz as above; f_{ce} is the electron gyrofrequency, taken to be 1.44 MHz which corresponds to 200 km above AGO-P1; and θ is the angle between the wavevector of the whistler wave and the earth's magnetic field. The wave is incident on this boundary from the ionosphere, the side with the larger index of refraction. Hence total internal reflection is a possible outcome. The condition for total internal reflection not to occur, i.e., the condition for the wave to refract into the atmosphere, is

$$n^2 \sin^2\alpha < 1 \tag{2}$$

where α is the angle between the wavevector and the normal to the interface, which is the vertical. The angles θ and α are related to each other and to the dip angle of the magnetic field ($\lambda \approx 77°$ at AGO-P1) by

$$\theta = \lambda + \alpha - 90°. \tag{3}$$

Substituting (1) and (3) into (2) determines a condition for the waves to reach the ground. This condition defines a narrow cone of angles near vertical incidence for which the whistler mode waves penetrate into the atmosphere; wave vectors whose angles with the vertical lie outside this "transmission cone" do not reach

the ground. For the parameters given above which are appropriate for AGO-P1, the half-width of the transimission cone is 2.6° at 8 kHz, 6.0° at 40 kHz, and 8.3° at 80 kHz. Modeling the ionosphere-atmosphere interface as a plane boundary is good enough to help determine whether propagation effects provide a plausible explanation for LF cutoff auroral hiss; however, future work should explore more complex models of the ionosphere-atmosphere interface which are needed to more accurately model the frequencies considered here, which range from 8 to 80 kHz (wavelengths of 4–40 km).

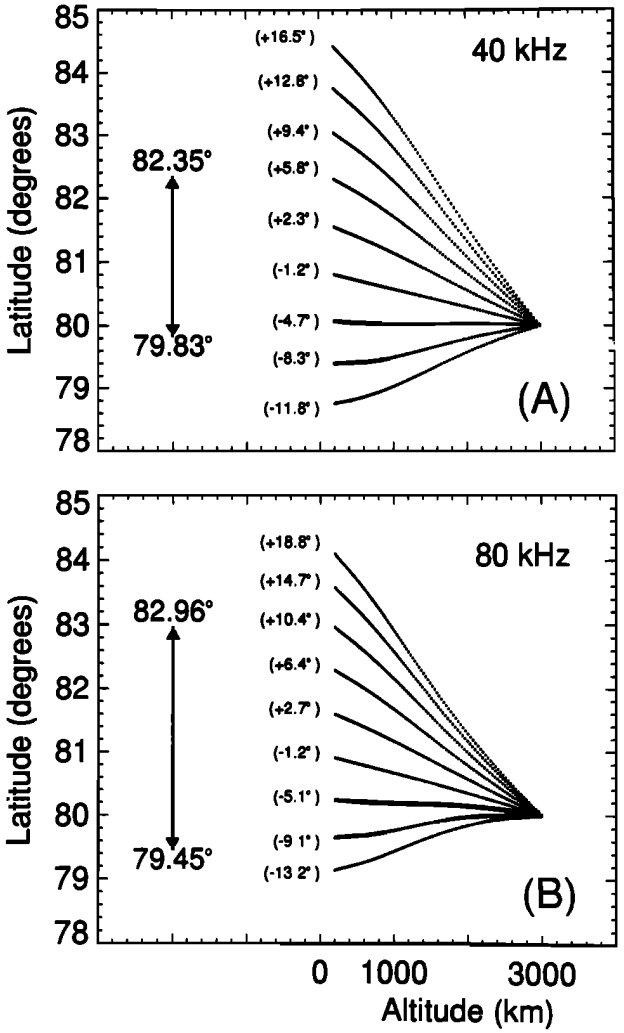

Figure 6. Ray tracing calculations for propagation of (a) 40 and (b) 80 kHz auroral hiss launched from a hypothetical source at 3000 km altitude and 80° invariant latitude. Seven example whistler mode rays were traced from 3000 to 200 km using a magnetopheric whistler ray tracing code; the angles between the wave vectors and the vertical at the 200 km end point are indicated in parintheses. On the basis of these angles and a simple Snell's law model for transmission of the waves into the atmosphere, the rays over the ranges of latitude indicated by dark vertical bars would penetrate to the ground (79.83°–82.35° for the 40 kHz waves; 79.45°–82.96° for the 80 kHz waves). Ignoring effects of subionospheric propagation one would infer from this model that in some average sense, 28% of the ground observers who detect auroral hiss in this latitude range would detect 80 kHz waves but not 40 kHz waves.

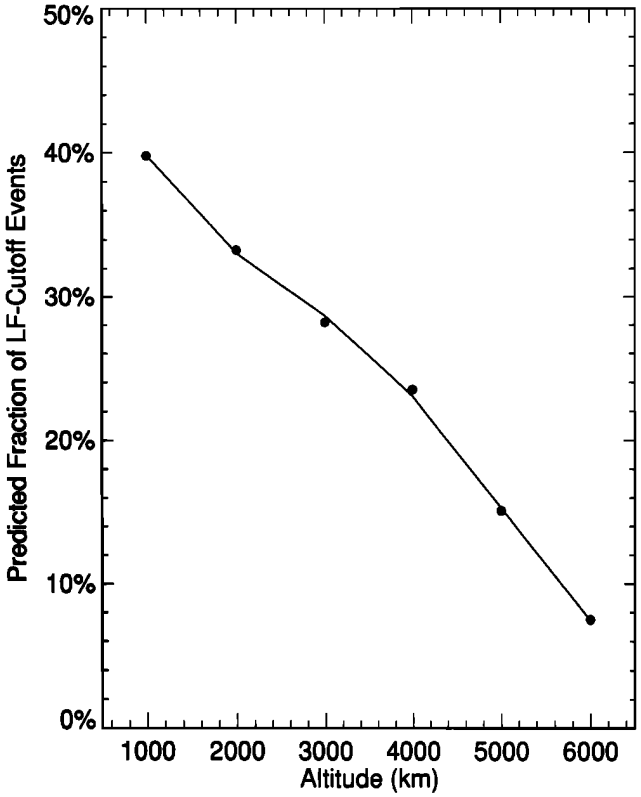

Figure 7. Model predictions of the percentage of LF cutoff events as a function of the LF auroral hiss source altitude, which is the most sensitive factor affecting this prediction. The observed percentage of LF cutoff events at AGO-P1, 14–36%, corresponds to altitudes of 2000–5000 km, which agrees well with the altitude range for which the electron gyrofrequency or plasma frequency is typically in the range 50–100 kHz.

Figure 6 shows the results of this model for 40 kHz (Figure 6a) and 80 kHz (Figure 6b) auroral hiss. The source altitude h = 3000 km, and for each frequency, seven waves are launched from the field line corresponding to 80° magnetic latitude. The waves are launched in the meridional plane at angles from the magnetic field ranging from −30° to +30°. Figure 6 shows how the ray paths diverge from each other in altitude-invariant latitude space while propagating from 3000 to 200 km. Numbers in parintheses indicate the angles that the wavevectors make with the vertical at the 200 km endpoints of the ray traces. Finally, the dark vertical bars indicate the range of latitudes for which the wavevectors at 200 km fall within the transmission cone for the appropriate frequency. In this rough propagation model, the 40 kHz rays originating at 3000 km altitude and 80° magnetic latitude can reach the ground for the latitude range 79.83°–82.35°; the corresponding latitude range for the 80 kHz waves is 79.45°–82.96°. There is a range of latitudes for which the 80 kHz waves penetrate

to the ground but the 40 kHz waves do not. We associate this range of latitudes with LF cutoff hiss. Taking the ratio of the range of latitudes for which only 80 kHz waves reach the ground to the total range of latitudes for which either 40 or 80 kHz waves reach the ground, we get 28%, which we interpret as the approximate percentage of LF cutoff auroral hiss events predicted by the simple model. (The predicted percentage varies little with geomagnetic latitude, so a set of rays traced from a single latitude, 80° in this case, monitored by an ensemble of points on the ground, is equivalent to the experimental situation which consists of a single ground station at 80° sampling waves from an ensemble of source latitudes.)

Many parameters affect the percentage of LF cutoff events predicted by the model, but the source altitude h is the most significant factor. Numerical calculations (not shown) establish that the geomagnetic latitude and reasonable variations in the electron density profile play a less significant role. Figure 7 shows model predictions of the percentage of LF cutoff events as a function of the source altitude. Altitudes of 2000–5000 km correspond to 14–36% LF cutoff events, the approximate observed percentage, depending on how the mixed spectral type events are counted. This range of altitudes agrees well with the altitude range for which the electron gyrofrequency or plasma frequency is typically in the range 50–100 kHz, and it agrees with the *Makita* [1979] direction finding observations suggesting that impulsive auroral hiss comes from directions close to those of the visible auroral forms.

Makita [1979] applied the propagation model primarily to VLF hiss. The application of the model to make predictions about LF cutoff auroral hiss suffers from at least three shortcomings. First, it does not account for subionospheric propagation. If the subionospheric propagation is not too different for 40 versus 80 kHz waves, the model has some validity despite this shortcoming. Second, the model likewise assumes that the altitude of the source or duct exit point does not vary significantly with frequency over the range 40–80 kHz. Third, the Snell's law model for computing the transmission cone is in principle valid only if the wavelength is long compared to the actual density gradient at the bottomside of the ionosphere, which is valid at VLF but not strictly valid at 80 kHz. We therefore interpret Figure 7 with caution, and extract qualitative rather than quantitative information from the model. The model provides strong evidence that the LF cutoff phenomenon can be explained as a wave propagation effect. The model suggests that the observed statistics of LF cutoff auroral hiss at AGO-P1 are consistent with LF whistler mode hiss originating at altitudes of 2000–5000 km, or ducted to that altitude from higher a altitude source by density irregularities or horizontal density gradients. To quantify this conclusion will require a significantly better model, including in particular a more accurate treatment of the interface between the ionosphere and atmosphere.

4. Conclusions

Antarctic AGO measurements reveal occurrence statistics and spectral characteristics of LF impulsive auroral hiss emissions. The occurrence rates of these LF emissions at ~80° invariant latitude have diurnal and seasonal dependencies that approximately agree with previous observations of VLF and LF hiss at auroral latitudes, except for a secondary peak in the austral summer months observed at AGO-P1 in 1994 but not 1995, whose significance needs to be evaluated based on future data. More significant are the AGO observations of the spectrum of the auroral hiss at LF, which cannot be observed at northern hemisphere sites or manned Antarctic stations due to man-made interference. We identify two spectral types of LF impulsive auroral hiss: normal events, in which the power spectral density is a decreasing function of frequency throughout the LF band, presumably peaking in the VLF band below the frequency range of the LF/MF/HF receiver; and LF cutoff events, for which the power spectral density peaks in the LF band with little or no power at VLF. Out of a large sample of LF impulsive auroral hiss events observed at AGO-P1, 64% are the normal type, 14% are the LF cutoff type, and 22% are a mixture of both.

A version of the *Makita* [1979] model for propagation of auroral hiss from a high-altitude source to the ground was developed in order to obtain a rough idea whether this type of model can explain the observed occurrence statistics of the different types of LF impulsive auroral hiss. The results indicate that LF cutoff auroral hiss can be explained by propagation effects and suggest that the observed LF cutoff occurrence statistics are consistent with LF impulsive auroral hiss originating at or ducted to altitudes of 2000–5000 km. A better model combined with statistics of LF cutoff hiss from multiple stations may allow a stronger conclusion concerning the source altitude and propagation of the high-latitude LF auroral hiss observed at ground level. Future case studies involving other AGO instruments such as the imaging riometer and optical imager also may improve understanding of the generation and propagation of LF cutoff auroral hiss.

Acknowledgments. The authors thank the AGO investigator team, especially H. Fukunishi and L. Lanzerotti, for providing their data in support of this paper. The authors also thank Dave Lauben for providing the VLF ray tracing code with instructions and Eric Lund for help modifying it to run on our computers. The Antarctic Support Associates and Lockheed-Martin Corporation are to be thanked for their long-term support of the automatic geophysical observatories which were critical to this study. This research was supported by National Science Foundation grants OPP-9317621 to Dartmouth College, OPP-9529177 to the University of Maryland, and University of Maryland subcontract Z329101-A to Stanford University.

The editor thanks Forrest Mozer and Craig Kletzing for their assistance in evaluating this paper.

References

Burtis, W.J., *User's Guide to the Stanford VLF Ray Tracing Program*, Radioscience Lab. Rep., Stanford Univ., Stanford, Calif., 1974.

Dowden, R.L., Low-frequency (100 kHz) radio noise from the aurora, *Nature*, suppl., **184**, 803, 1959.

Ellyett, C.D., Radio noise of auroral origin, *J. Atmos. Terr. Phys.*, *31*, 671–682, 1969.

Ergun, R.E., E. Klementis, C.W. Carlson, J. McFadden, and J.H. Clemons, Wavelength measurement of auroral hiss, *J. Geophys. Res.*, *96*, 21299, 1991.

Helliwell, R.A., *Whistlers and Related Ionospheric Phenomena*, Stanford Univ. Press, Stanford, Calif., 1965.

Inan, U.S., and T.F. Bell, The plasmapause as a VLF wave guide, *J. Geophys. Res.*, *82*, 2819, 1977.

Jorgensen, T.S., Morphology of VLF hiss zones and their correlation with particle precipitation events, *J. Geophys. Res.*, *71*, 1367, 1966.

Jorgensen, T.S., Interpretation of auroral hiss measured at OGO 2 and at Byrd Station in terms of incoherent Cerenkov radiation, *J. Geophys. Res.*, *73*, 1055, 1968.

Kellogg, P. J., and S. J. Monson, Radio emissions from the aurora, *Geophys. Res. Lett.*, *6*, 297, 1979.

Kimura, I., Effects of ions on whistler mode ray tracing, *Radio Sci.*, *1*, 269–283, 1966.

LaBelle, J., Radio noise of auroral origin, 1968–1988, *J. Atmos. Terr. Phys.*, *51*, 197, 1989.

LaBelle, J., and A.T. Weatherwax, Ground-based observations of LF/MF/HF radio waves of auroral origin, in *Proceedings of the 1992 Cambridge Workshop in Geoplasma Physics*, edited by T. Chang, p. 223, Scientific, Cambridge, Mass., p. 223, 1993.

LaBelle, J., A. Weatherwax, M. Trimpi, R. Brittain, R. Hunsucker, and J. Olson, The spectrum of LF/MF/HF radio noise at ground level during geomagnetic substorms, *Geophys. Res. Lett.*, *21*, 2749, 1994.

LaBelle, J., S. Shepherd, and M.L. Trimpi, Further observations of auroral MF burst, to appear in *J. Geophys. Res.*, *102*, 22221, 1997.

Maggs, J.E., Coherent generation of VLF hiss, *J. Geophys. Res.*, *81*, 1707, 1976.

Makita, K., VLF/LF hiss emissions associated with aurora, *Mem. Natl. Inst. Polar Res., Ser. A*, no. 16, 1, 1979.

Morgan, M.G., Wide-band observations of LF hiss at Frobisher Bay, *J. Geophys. Res.*, *82*, 2377, 1977a.

Morgan, M.G., Auroral hiss on the ground at L=4, *J. Geophys. Res.*, *82*, 2387, 1977b.

Morioka, A., and H. Oya, Emissions of plasma waves from VLF to LF ranges in magnetic polar regions—New evidence from the EXOS-C satellite, *J. Geomagn. Geoelectr.*, *37*, 263, 1985.

Mosier, S.R., and D.A. Gurnett, VLF measurements of the Poynting flux along the geomagnetic field with the Injun-5 satellite, *J. Geophys. Res.*, *74*, 5675, 1969.

Rosenberg, T.J., and J.H. Doolittle, Studying the polar ionosphere and magnetosphere with automatic geophysical observatories: The U.S. program in Antarctica, *Antarctic J. U.S.*, *29*, no. 5, 347, 1994.

Sato, N., S. Kokubun, and T. Saemundsson, Geomagnetic conjugacy of 30 kHz auroral hiss emissions observed at L=6.1, *J. Geophys. Res.*, *92*, 6159, 1987.

Sazhin, S.S., K. Bullough, and M. Hayakawa, Auroral hiss: A review, *Planet. Space Sci.*, *41*, 153, 1993.

Singh, D.P., and B. Singh, Propagation characteristics of ground observed VLF waves after emerging from the ducts in the ionosphere, *Ann. Geophys.*, *34*, 113–118, 1978.

Weatherwax, A.T., J. LaBelle, M.L. Trimpi, and R. Brittain, Ground based observations of radio emissions near $2f_{ce}$ and $3f_{ce}$ in the auroral zone, *Geophys. Res. Lett.*, *20*, 1447, 1993.

Weatherwax, A.T., J. LaBelle, and M.L. Trimpi, A new type of auroral radio emission at 1.4-3.7 MHz observed from the ground, *Geophys. Res. Lett.*, *21*, 2753, 1994a.

Weatherwax, A.T., J. LaBelle, and M.L. Trimpi, A comparison of electromagnetic noise at ground based radio observing sites, *Antarctic J. U.S.*, *29*, no. 5, 365–366, 1994b.

Yamamoto, T., On the amplification of VLF hiss, *Planet. Space Sci.*, *27*, 273, 1979.

U.S. Inan, Department of Electrical Engineering, Stanford University, Stanford, CA 94305.

J. LaBelle, J. Perring, M. L. Trimpi, and E. Walsh, Department of Physics and Astronomy, Dartmouth College, 6127 Wilder Laboratory, Hanover, NH 03755.

A.T. Weatherwax, Institute for Physical Science and Technology, University of Maryland, College Park, MD 20742.

(Received December 8, 1997; revised May 5, 1998; accepted May 5, 1998.)